Published in Applied Physics Letters 83, issue 3, 584-586, 2003
which should be used for any reference to this work

Propagation of the electromagnetic field in fully coated near-field optical probes

L. Vaccaro,[a] L. Aeschimann,[b] U. Staufer, H. P. Herzig, and R. Dändliker
Institute of Microtechnology, University of Neuchâtel, Rue A.-L. Breguet 2 and Rue Jaquet-Droz 1, 2000 Neuchâtel, Switzerland

Fully metal-coated near-field optical probes, based on a cantilever design, have been studied theoretically and experimentally. Numerical simulations prove that these structures allow nonzero modal emission of the electromagnetic field through a 60-nm-thick metallic layer, that is opaque when deposited on flat substrates. The far-field intensity patterns recorded experimentally correspond to the ones calculated for the fundamental and first excited LP modes. Moreover, this study demonstrates that a high confinement of the electromagnetic energy can be reached in the near-field, when illuminated with radially polarized light. Finally, it was verified that the confinement of the field depends on the volume of the probe apex.

Nearly 20 years of intensive research in near-field optical microscopy have produced satisfying results in imaging and subwavelength resolution.[1]

The key element is the near-field optical probe that rasters the object field in the evanescent region. Various concepts have been adopted to produce near-field optical probes. Among them we only cite the ones that have been most widely employed in this field. They are produced by chemical etching or heating and pulling a monomode silica fiber, resulting in a cone that is subsequently metal-coated in such a way as to leave a small aperture at the cone apex.[2,3] However, the reproducibility of the optical characteristics of such probes cannot be guaranteed in a production procedure.

Several one-by-one postprocessing alternatives have been proposed and applied with success, nevertheless they are very expensive and time consuming.[4,5]

Recently a very innovative design that combines near-field optical probes with a cantilever [atomic force microscopy–scanning near field optical microscopy (SNOM) hybrid probes] has been proposed. In this approach, the probes comprise a 12 μm high amorphous SiO_2 conical near-field tip on a silicon cantilever. Transmission electron microscopy reveals a 60-nm-thick polycrystalline iridium layer, that completely covers the quartz tip.[6] Iridium coated cantilever probes present interesting mechanical and optical features: the hardness of the material guarantees high mechanical damage threshold, potentially increasing the lifetime of the probes. Optically, this metal has also a satisfying behavior.[7] The probes have been used to illuminate the near-field of fluorescently labeled single molecules, yielding a resolution of 32 nm.[8]

Far-field characterization of the probes emission has been performed by coupling radiation of a linearly polarized laser (He–Ne @ 632 nm) in the cantilevers. The pattern displayed in Fig. 1(a) has been recorded in a configuration in which the polarizers positioned before the cantilever entrance (p) and after its apex (a) are parallel. The intensity pattern recorded in this case corresponds to the fundamental linearly polarized mode LP_{01}. The radiation emitted presents a polarization state parallel to the one of the field that has been coupled in the probe. In Fig. 1(b) is shown the intensity pattern recorded when the polarizers (p) and (a) are orthogonally oriented. This pattern can be generated by the superposition of two first excited modes LP_{11} orthogonally oriented leading to a radial polarization state, compatible with the polarizers configuration. It is worth remarking that, even if we couple only a single mode radiation in the cantilever, other excited modes can be generated at its entrance that is not specifically mode matched.

In this letter, we present a theoretical study of the propagation and of the emission properties of the probes. The goal was to study the mechanism that allows the electromagnetic field to penetrate such a thick metal layer, which is opaque when deposited on a flat surface. The theoretical study of the electromagnetic field propagation has been carried out taking into account different polarized modes, that, under specific conditions, can display very pronounced emission characteristics. It is proven that this kind of structure, when employed in the near-field, presents a very confined emission characteristics, and that the field confinement is generated only when radially polarized radiation is coupled in it. Moreover,

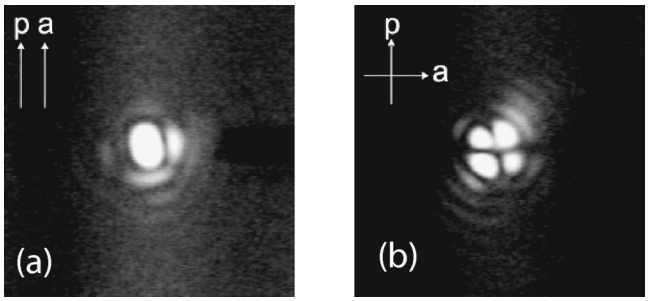

FIG. 1. Far-field energy pattern recorded experimentally when the polarizer and the analizer are parallel (a) or orthogonal (b).

[a]Electronic mail: luciana.vaccaro@unine.ch
[b]Also at: the Swiss Center for Electronics and Microtechnology CSEM, Rue Jaquet-Droz 1, 2007 Neuchâtel, Switzerland.

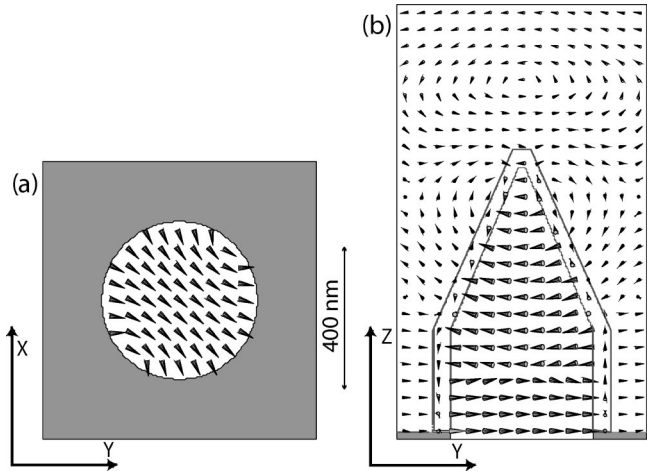

FIG. 2. Normalized direction of the E field of the mode LP_{01} at the entrance of the waveguide (a) and along the propagation direction (b).

the computational results show that the geometrical parameters of the field confinement is highly dependent on the radius of the apex.

The theoretical calculations, based on the finite integration code MAFIA4 (CST, Darmstadt, Germany), were implemented on a structure of silica ($\epsilon = 2.16$) completely coated by a 60-nm-thick layer of iridium (@ $\lambda = 632$ nm, $\epsilon = -14.64 + i22.85$). (The complex value of the dielectric constant was measured by spectroellipsometry on a silicium substrate which was coated simultaneously with the SNOM probe.) The silica structure is composed of a 300 nm high cylinder (radius 200 nm) covered by a 450 nm high cone of the same radius. In the general case, the probe apex diameter is 60 nm. For the calculations, the geometry that has been employed is placed in a volume of $0.7 \times 0.7 \times 1.2\ \mu m^3$ for the first propagating mode and $1.4 \times 1.4 \times 1.2\ \mu m^3$ for the second one, as shown in Figs. 2 and 3. In both cases the volume is discretized in mesh cells of $7 \times 10 \times 10\ nm^3$.

In Figs. 2(a) and 3(a) the two different eigenmodes of the waveguide are displayed. They are separately coupled into the waveguide and the resulting electric field directions are displayed in Figs. 2(b) and 3(b), respectively. The mode displayed in Fig. 2(a) is classified as a linearly polarized mode LP_{01} characterized by a polarization direction at 45° in the (x,y) plane. In this case, one can see that the electric field propagating in the structure remains orthogonal to the propagation direction through the entire probe length [see Fig. 2(b)]. The field undergoes a cutoff when the cone radius becomes smaller than 100 nm, resulting in a field emission on opposite sides of the cone.

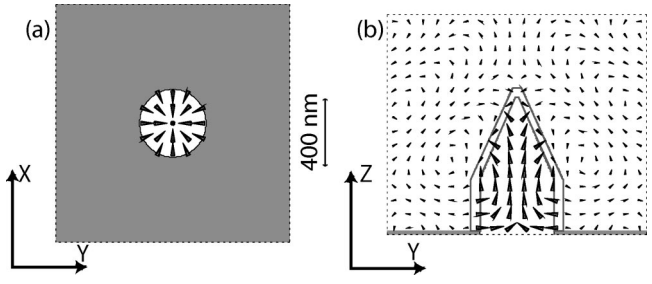

FIG. 3. Normalized direction of the E field of the mode LP_{11} at the entrance of the waveguide (a) and along the propagation direction (b).

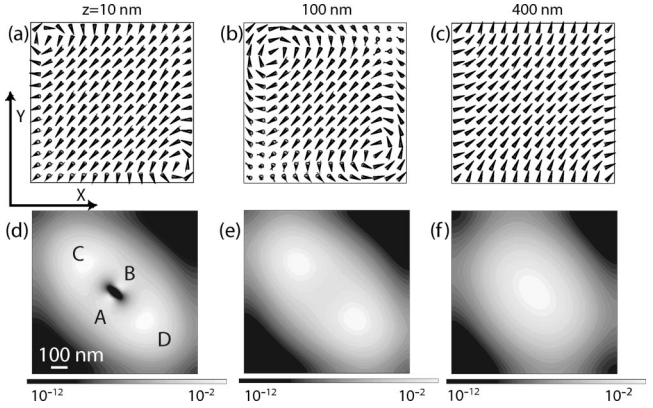

FIG. 4. E-field direction (a), (b), (c) and intensity countour plot (d), (e), (f) for LP_{01} mode at different heights above the probe apex.

The mode displayed in Fig. 3(a) can be obtained by the superposition of two LP_{11} modes that are horizontally and vertically polarized in the waveguide. It is characterized by a radial polarization at the entrance of the waveguide and by a nonzero z component of the electric field when propagating into the cone. These propagating conditions allow the coupling of bulk plasmons in the metal cladding, and induce there stable waveguiding conditions. It is worth pointing out that in the conical region of the probe [Fig. 3(b)] the z component of the electric field becomes dominant.

By observing the field orientation for both modes in (x,y) planes at different distances from the probe apex we can understand the different behaviors that differentiate the two modes in the near-field.

In the case of the LP_{01} mode, Figs. 4(a) and 4(b) display in the near-field two vortices in the corner of the two images, that represent polarization discontinuities in the (x,y) plane. As the observation plane withdraws from the tip apex, the vortices approach each other along the diagonal until they annihilate in the far-field (400 nm). At that distance the polarization direction is the same as at the injection into the waveguide.

From the intensity pattern displayed in Figs. 4(d), 4(e), and 4(f), one can see the two lobes labeled with C and D originating from the cone side. They peak at very high intensity at a distance of above the tip apex and, at larger distances, tend to merge into a single diffracted spot. At 1 μm the spot becomes perfectly circular (data not shown). This result agrees with the far-field intensity pattern obtained experimentally when the axis of the polarizer and the analyzer are parallel.

The origin of the two smaller spots of high intensity [A and B in Fig. 4(d)], visible only in the near-field region, can be explained by the depolarization effect.[9] This effect is generated when a field E_0 is coupled into a small volume of matter, giving rise to a depolarization field E_d. The resulting internal field is $E_{\text{int}} = E_0 + E_d$ and it has to fulfill the boundary conditions required by the Maxwell equations at the dielectric-air interface. When the field E_0 is polarized in a direction parallel to the interface plane, the depolarization field induces a strong variation of the field intensity along the direction of polarization. As previously mentioned, the two larger zones of high intensity (C, D) correspond to the propagation of the light that leaks from the sides of the cone.

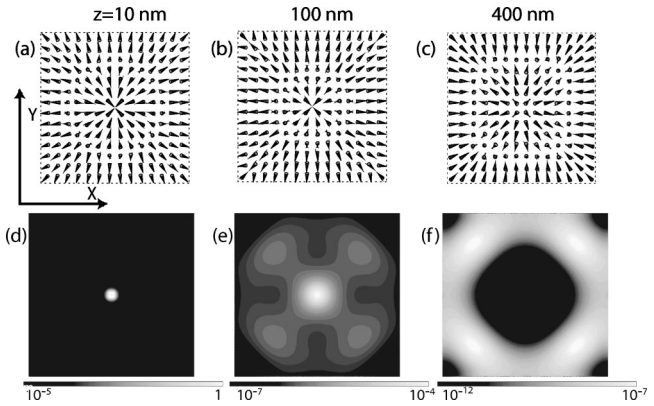

FIG. 5. E-field direction (a), (b), (c) and intensity contour plot (d), (e), (f) for LP_{11} mode at different heights above the probe apex.

Along this direction, indeed, the incident field already satisfies the boundary conditions at the protrusion edges that are parallel to the incident field. Hence, no depolarization effect is visible in this direction.

We want to emphasize that the depolarization effect has been described only when a dielectric medium is inserted in an infinite volume of metal.[10] In the present work we found evidence of the depolarization effect when a thin layer of metal is deposited on the dielectric interface.

From Figs. 5(a), 5(b), and 5(c) one can see that the electric field preserves a strong axial component in the near and mean-field for the LP_{11} mode. The energy of the electromagnetic field calculated at 10 nm above the probe apex shows a very distinct single spot with a full width at half maximum (FWHM) of 114 nm. The spot evolves into a larger one surrounded by four lobes that become dominant in the far-field (400 nm). The intensity pattern obtained at a distance of 400 nm above the probe apex is comparable to the one recorded experimentally in the far-field when the polarizer and the analyzer are orthogonal. In this case the E field is perpendicular to the plane of discontinuity. Hence, for the LP_{11} mode the depolarization effect is not visible in (x,y) planes. Moreover, thanks to the waveguiding conditions in the metallic layer, this polarization state induces a strong field confinement in the small volume of the probe apex, that results in a subvawelength confinement in the near-field and that depends on the size of volume of the protrusion.

The difference of behavior between the two propagating modes has been observed experimentally[11] and studied theoretically in pure dielectric structures in analogous configurations.[12]

A parametric study as a function of the diameter of the probe apex demonstrates that the confinement depends highly on the volume of the protrusion. The FWHM of the intensity of the electromagnetic field has been calculated for probe apex diameters of 6, 60, and 200 nm and is reported in Table I. The table clearly shows that a smaller geometry results in a higher confinement of the field. In more detail, a superresolved spot of 42 nm at FWHM is obtained with a probe of 6 nm, but even with a probe of 200 nm we still obtain a subwavelength confinement that corresponds to 214 nm (FWHM) of the intensity of the electromagnetic field.

TABLE I. FWHM of the energy distribution of the electromagnetic field calculated at a distance of 10 nm above the probe apex for the mode LP_{11}.

Apex diameter	6 nm	60 nm	200 nm
FWHM	42 nm	114 nm	240 nm

The propagation of two different modes shows that subwavelength confinement of the electromagnetic field occurs when the E field gets a strong component along the axis of the probe.[13] In particular, the two modes show a very distinct behavior when coupled into the probe, in analogy to what was previously found in the near-field optical detection of electric fields emerging from gratings.[14] Moreover, the full width at half maximum of the field is highly dependent on the size of the final protrusion. We expect that the optical resolution obtained employing these probes in near-field optical microscopy has the same dependence.

R. Germann, IBM Zurich, is greatly acknowledged for the spectroellipsometric characterization of the metal layers. L.V. thanks C. Ciuti, Ph. Lalanne, and M. Saba for stimulating discussions. Stimulating discussions with our industrial partners Nanoworld AG and WiTec GmbH are gratefully acknowledged as well. This work has been supported by the Swiss National Science Foundation and the program TOP NANO 21.

[1] M. Ohtsu and H. Hori, *Near-Field and Nano-Optics* (Kluwer Academic, New York, 1999).
[2] P. Lambelet, A. Sayah, M. Pfeffer, C. Philipona, and F. Marquis-Weible, Appl. Opt. **37**, 7289 (1998).
[3] E. Betzig and J. K. Trautman, Science **251**, 1468 (1991).
[4] J. A. Veerman, A. M. Otter, L. Kuipers, and N. F. van Hulst, Appl. Phys. Lett. **72**, 3115 (1998).
[5] O. Sqalli, M. P. Bernal, P. Hoffmann, and F. Marquis-Weible, Appl. Phys. Lett. **76**, 2134 (2000).
[6] L. Aeschimann, T. Akiyama, U. Staufer, N. F. De Rooij, L. Thiery, R. Eckert, and H. Heinzelmann, J. Microsc. **209**, 182 (2003).
[7] E. D. Palik, *Handbook of Optical Constants of Solids*, 3rd ed. (Academic, New York, 1998).
[8] R. Eckert, J. M. Freyland, H. Gersen, H. Heinzelmann, G. Schürmann, W. Noell, U. Staufer, and N. F. de Rooij, Appl. Phys. Lett. **77**, 3695 (2000).
[9] C. Kittel, *Introduction to Solid State Physics* (Wiley, New York, 1986).
[10] O. J. F. Martin and M. Paulus, J. Microsc. **295**, 147 (2001).
[11] C. Adelmann, J. Hetzler, G. Scheiber, T. Schimmel, M. Wegener, H. B. Weber, and H. von Lohneysen, Appl. Phys. Lett. **74**, 179 (1999).
[12] O. J. F. Martin, C. Girard, and A. Dereux, J. Opt. Soc. Am. A **13**, 1801 (1996).
[13] P. M. Adam, P. Royer, R. Laddada, and J. L. Bijeon, Appl. Opt. **37**, 1814 (1998).
[14] A. Nesci, R. Dändliker, M. Salt, and H. P. Herzig, Opt. Commun. **205**, 229 (2002).